Eur. Phys. J. Special Topics **223**, 1265–1277 (2014)
© EDP Sciences, Springer-Verlag 2014
DOI: 10.1140/epjst/e2014-02190-2

THE EUROPEAN PHYSICAL JOURNAL SPECIAL TOPICS

Regular Article

Modular approach for modeling cell motility

F. Ziebert[1,a] and I.S. Aranson[2,3,b]

[1] Theoretische Physik I, Universität Bayreuth, 95440 Bayreuth, Germany
[2] Materials Science Division, Argonne National Laboratory, 9700 S. Cass Avenue, Argonne, IL 60439, USA
[3] Engineering Sciences and Applied Mathematics, Northwestern University, 2145 Sheridan Road, Evanston, IL 60202, USA

Received 20 December 2013 / Received in final form 14 April 2014
Published online 12 June 2014

Abstract. Modeling cell movement is a challenging task since the motility machinery is highly complex. Moreover, there is a rather broad diversity of different cell types. In order to obtain insights into generic features of the motility mechanisms of several distinct cell types, we propose a modular approach that starts with a minimal model, consisting of a phase field description of the moving cell boundary and a simplified internal dynamics. We discuss how this starting point can be extended to increase the level of detail, and how the internal dynamics "module" can be changed/adjusted to properly model various cell types. The former route allows studying specific processes involved in cell motility in the framework of a self-organized moving domain, and the latter might permit to put different cellular motility mechanisms into a unified framework.

1 Introduction

Observing the plethora of moving cell types, from shape-preserving and fast moving keratocytes to the unsteady, searching motion of fibroblasts, to leukocytes and amoebae, ever changing shape and direction, one might wonder whether it was possible to put this diversity into a unifying framework. The cells share common features, though: they need a (usually cytoskeleton-related) protrusion force, adhesion to transfer momentum to the substrate, and a mechanism of retraction [1,2]. From the biological perspective, the nature of these processes may be rather diverse: protrusion can be due to ratcheting of actin polymerization [3], actin polymerization waves [4], motor-generated stresses [5], or local swelling of the cytoskeleton gel [6], to name just the most common mechanisms. Adhesion can be integrin-based [7,8] as for the most epithelial cells, rely on nonspecific adhesion (i.e. friction, as for amoebae like dictyostelium devoid of focal adhesion), and some cells can even switch between both adhesion types, like dendritic cells [9]. Retraction may be motor-induced, or again rely on different mechanisms, for instance on gel collapse as proposed for nematode sperm cells [10].

[a] e-mail: fziebert@gmail.com
[b] e-mail: aronson@anl.gov

From the physics and active matter points of view, however, this diversity shares common features: (i) the establishment of a self-organized distributed force – propulsive and/or retractile. It includes the force transfer to the substrate and acts on a soft interface, the cell membrane, aiming to locally propel it forwards. (ii) A mechanism, e.g. motor contraction [11], that breaks the global symmetry and leads to a self-sustained motion (more or less stable, depending on the cell type). Importantly, it has been shown that fragments of motile cells, devoid of the nucleus and most organelles and hence with substantially reduced biochemical regulation, can still display a cell-like self-sustained motion [12,13] if instead of (ii) the symmetry is broken externally. This strengthened the view that the motility machinery is self-organized and led to an increasing interest in modeling cell motility within the physics community.

First steps in modeling were descriptive, like the graded protrusion model [14], followed by one-dimensional or fixed shape models [5,15–17] to test conceptional ideas and to extract generic features. For these approaches we refer to the very recent review Ref. [18]; rather, we will focus here on approaches that treat the cell's shape self-consistently. This is needed since the cell's shape is determined dynamically [19] and propulsion forces are typically located at or near the membrane. Hence the dynamics of the membrane enters the problem as an additional degree of freedom, and a complex one due to global constraints like area/volume conservation, tension, etc. The phase field method [20–22], or related approaches like level set, offers a powerful and elegant way to implement moving boundaries, and has been successfully applied to model motile cells [23–28].

We propose here a modular approach that is based on a minimal model [24] that only describes a closed interface (the cell membrane) with a simplified internal dynamics (related to the actin cytoskeleton) and is described in Sect. 2. The model allows for a modular approach in two respects: first, we discuss how it can be extended to increase the level of detail, as exemplified in Sect. 3 for the substrate-dependent adhesion dynamics and for incorporating membrane tension. Note that such, more specific, processes can be added one by one and investigated in the framework of a self-organized moving domain. Second, we discuss in Sect. 4 how the internal dynamics "module" can be changed/adjusted to model properly various cell types. This is similar in spirit to Ref. [29], and might permit to combine and compare different cellular motility mechanisms within a unified framework.

2 Minimal model: An interface coupled to simple internal actin dynamics

The minimal model that we proposed in Ref. [24] consists of a closed interface – that can be identified with the cell's membrane – and a simplified acto-myosin cytoskeleton dynamics in the interior. Since it is rather difficult to evaluate numerically moving boundary conditions at the interface and match them to the interior of the cell (see, e.g. [30]), the interface is described implicitly by a *phase field*: an auxiliary field, $\rho(x, y; t)$, assuming $\rho = 1$ inside the cell and $\rho = 0$ outside (other parameterization is possible, of course). The phase field varies smoothly between 0 and 1, and the interface can be defined by $\max(|\nabla\rho|)$ or by a fixed value of ρ (e.g. $\rho = \frac{1}{2}$).

The simplest phase field implementation of an interface is given by

$$\partial_t \rho = D_\rho \Delta\rho - (1-\rho)(\delta-\rho)\rho\,. \tag{1}$$

The first term on the r.h.s. determines the width of the interface and the second one is the variational derivative $\frac{\delta F}{\delta \rho}$ of a model "free energy" $F(\rho)$ that has a double well structure with minima at $\rho = 0$ and 1, cf. Fig. 1a. The value of δ determines which of

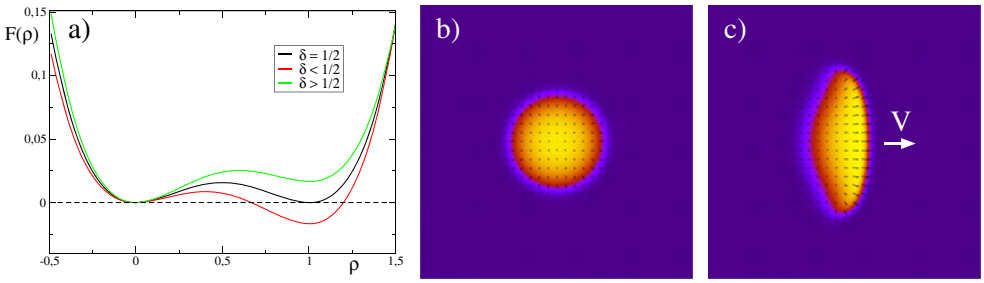

Fig. 1. a) Free energy $F(\rho) = \int^{\rho}(1-\rho')(\delta-\rho')\rho' d\rho'$ associated to the phase field ρ. For $\delta = \frac{1}{2}$ (black curve) both "phases", 0 and 1, have the same energy. Otherwise one of the phases is preferred resulting in contraction (the outside $\rho = 0$ is preferred, green curve) or spreading of the cell (the inside $\rho = 1$ is preferred, red curve). Panel b) shows a stationary and stable solution of a symmetric immobile cell, while c) shows a polarized cell moving with a constant speed. Both are results of Eqs. ((5), (6)) for same parameters. Arrows show the actin orientation field $\mathbf{p}$.

these two "phases" (the inside, $\rho = 1$, or the outside, $\rho = 0$) is preferred. For $\delta = \frac{1}{2}$ both phases have the same free energy and hence the planar interface is stationary [cf. the black curve in Fig. 1a]. Note that solving Eq. (1) in one dimension leads to the typical tanh-solution

$$\rho_0(x) = \frac{1}{2}\tanh\left(\frac{x - x_0}{2\sqrt{2D_\rho}}\right) + \frac{1}{2} \tag{2}$$

known from the Ginzburg-Landau theory, where x_0 is the position of the interface connecting the phases 0 and 1. An evolution equation for a circular "droplet" of radius R, large compared to the interface width i.e. with $R \gg 1/\sqrt{D_\rho}$, can be obtained asymptotically by using the front solution given by Eq. (2) in polar coordinates (r, θ). Substitution in the form $\rho_0(x, y, t) = \rho_0(r - R(t))$ into Eq. (1), and applying the solvability condition with respect to $\partial_r \rho_0$, one obtains that the radius of the droplet R evolves according to (cf. the so-called Maxwell rule)[1]

$$\frac{dR}{dt} = -\frac{D_\rho}{R} - \sqrt{2D_\rho}\left(\delta - \frac{1}{2}\right). \tag{3}$$

Thus, the droplet shrinks for $\delta > \frac{1}{2}$ and spreads for $\delta < \frac{1}{2}$.

External factors (e.g. polymerization forces in the cytoskeleton) will tilt the potential and hence one of the two phases will be preferred at the cost of the other phase. As an example, for keratocytes and other cells that do not change their area/volume in the course of movement, area conservation can be implemented as a global constraint:

$$\delta[\rho] = \frac{1}{2} + \mu\left[\int \rho\, dx\, dy - V_0\right]. \tag{4}$$

Here μ is the stiffness of the area constraint and the term in brackets is the difference of the actual area and the prescribed area V_0. If, for instance, the area is too small, the resulting $\delta < \frac{1}{2}$ will lead to an extension of the phase $\rho = 1$ (cf. the red curve in Fig. 1 and Eq. (3)), i.e. the cell will spread to restore the prescribed V_0.

[1] In the derivation we used that in polar coordinates the Laplace operator $\partial_r^2 + r^{-1}\partial_r \approx \partial_r^2 + R^{-1}\partial_r$ for the front solution, Eq. (2).

The following advantages of the phase field approach can be identified: First, moving boundaries are treated self-consistently, so no re-meshing is needed as in other methods. Second, as the phase field is defined everywhere in the integration domain, the equation(s) can be considered on a two-dimensional double periodic domain, allowing for very effective solutions in Fourier space. Finally, and most importantly for modular modeling approaches, all couplings between the interface and other relevant fields (actin, motors, adhesion bonds, regulatory agents etc.) can be implemented in a simple way via the phase field and its derivatives:

- confinement of the constituents to the interior of the cell can be achieved by multiplying respective densities/terms by ρ (or powers thereof)
- localization of the constituents to an area close to the interface can be achieved by using $\nabla\rho$ (or powers thereof).

We so far have defined a closed interface – corresponding to a localized distribution of ρ – that we interpret as the membrane surrounding the cell (for more detailed descriptions of "real" cell membranes, cf. the discussion in Sect. 3.2). For the implementation of the acto-myosin cytoskeleton obviously one has multiple choices, also due to the fact that different aspects of actin-related motility can be expressed in various cell types in different ways. Descriptions of the actin cytoskeleton used so far include implementations via its associated flow field (active gel theories [31], Mogilner and coworkers [32]) or via several concentration fields (e.g. bundled vs. unbundled actin [23] or G-actin monomers and F-actin filaments). Here we will use a minimal phenomenological model for the averaged actin orientation field [24]; more detailed descriptions/different motility mechanisms are discussed in Sects. 3 and 4.

The actin network is described by a vector field, $\mathbf{p}(x, y; t)$. Its direction is the averaged orientation of actin[2], its absolute value a measure for the degree of orientation (for more information about macroscopic descriptions of polar liquid crystals cf. [31,33]). From the biological perspective, one can identify two major factors that determine the most important coupling mechanisms to the cell's membrane: 1) polymerization of actin filaments is governed by membrane-associated proteins (nucleators and regulators like WASP and Arp2/3). This is described by a source term, $\beta\nabla\rho$, in the dynamic equation for $\mathbf{p}$. 2) Actin filaments, polymerizing at the boundary, push against the membrane due to the ratcheting of added monomers [3]. This is described by an advective term, proportional to α, in the equation for the phase field ρ. Including in the $\mathbf{p}$-equation degradation of actin (with rate τ_1) and a diffusive/elastic-like term yields[3] the two coupled equations

$$\partial_t\rho = D_\rho\Delta\rho - (1-\rho)(\delta[\rho]-\rho)\rho - \alpha\mathbf{p}\cdot(\nabla\rho)\,, \tag{5}$$

$$\partial_t\mathbf{p} = D_p\Delta\mathbf{p} - \beta\nabla\rho\, - \tau_1^{-1}\mathbf{p}\,. \tag{6}$$

The model so far describes a cell where actin is nucleated normal to the membrane and continuously pushes, but is held back by the volume conservation. Being symmetric, the cell is not able to move, cf. Fig. 1b. The symmetry must be broken and the symmetry-broken, polarized state must be able to sustain itself dynamically. For keratocytes, recently it has been shown by Yam et al. [11] that myosin motors are

[2] Note that actin has a directionality, both due to the different polymerization rates at the barbed and pointed ends and due to the directionality of associated molecular motors such as myosin.

[3] As the phase field is zero outside the cell, a value of $\mathbf{p}$ outside the cell will not matter, i.e. will not change the dynamics. One can also add a term $-\tau_2^{-1}(1-\rho^2)\mathbf{p}$ that explicitly suppresses $\mathbf{p}$ outside the cell.

responsible for the symmetry breaking. This is due to two effects: first, motors induce local contraction. Second, both for keratocytes and their cellular fragments, motors facilitate the formation of an acto-myosin bundle at the rear.

The first effect, contraction, can be modeled by adding a term $-\sigma|\mathbf{p}|^2$ to Eq. (4) for $\delta[\rho]$. Motivated by active gel theories [31], this term describes actin contraction by motors, with an associated rate parameter σ. It is possible to refine this description, by accounting for the stress field explicitly, cf. the discussion in Sect. 4. The second effect, motor-induced bundling at the rear, can be modeled by adding a symmetry-breaking term $-\gamma\,[(\nabla\rho)\cdot\mathbf{p}]\,\mathbf{p}$ to the equation for $\mathbf{p}$. This term can be motivated by a simple motor dynamics [24] and breaks the $\pm\mathbf{p}$ reflection symmetry. It describes increased motor activity at the rear and suppression of polarization $\mathbf{p}$ by formation of an antiparallel bundle: note that, unlike nematic filament order, the polar order described by the vector $\mathbf{p}$ is reduced for an anti-parallel, contractile bundle.

While the bundling effect seems to be keratocyte-specific (and is indeed needed for a crescent-like shape), the contractile term should apply more generally. Either of these two terms can induce stable moving solutions: a representative moving state (with both motor-related terms present) is shown in Fig. 1c. Note that the parameters in Fig. 1b and c are the same, only for c) the initial condition was stronger polarized in the $+x$-direction: the system is bistable, in accordance with experiments on cell fragments [12,13]. In addition, the model self-consistently reproduces the prediction of the Graded Radial Extension model, proposed some time ago as a (purely descriptive) model for keratocytes in [14]: there the authors noted, that since the shape does not change, the velocity should be graded with a maximum at the middle of the moving front decreasing towards the sides of the cell. Examining the distribution of $\mathbf{p}$ in the steady moving state, Fig. 1c, and noting that the local velocity is proportional to $\mathbf{p}$ (cf. the advective term), shows that this is automatically the case.

Concluding this part, the presented model is minimal, self-consistent, and reproduces the main phenomenology of moving keratocyte-like cells. In addition, it allows to develop more complex (hence more realistic) models for different cell types, since it is modular in two ways: (1) More details on both the internal dynamics and the interface response can be included in a step-by-step fashion, as discussed in the next section. (2) Although the internal dynamics can be quite different for different cell types, the phase field approach allows to couple them conveniently to the interface, as discussed already above. Hence different motility mechanisms can be discussed within the same modeling framework, cf. Sect. 4.

3 Gradual complexity increase by modular approach

Now we discuss two examples how to extend the simple model framework towards a more realistic description, one focusing on the internal dynamics and the other one on the interface.

3.1 Example: Basic features of adhesion dynamics and substrate elasticity

Cell adhesion is a multi-stage process that involves interactions of several proteins forming complexes that link the internal actin cytoskeleton to the outside, the extracellular matrix (ECM). Moreover, the system is mechanosensitive, i.e. the formation of adhesion sites depends on forces, both external ones and generated by the cell. Finally, adhesion sites undergo maturation [7,8]. We restrict ourselves here to the most basic phenomenology of motility-related adhesion: namely, by employing rectified actin polymerization creating a pushing force close to the membrane, the cell can

propel itself forwards *only if* it locally adheres. In other words, the force has to be transferred to the substrate, as can be observed by traction force measurements for both spreading and crawling cells [34,35].

The simplest way to include basic features of adhesion is to make the propulsion, i.e. the advective term $\alpha\mathbf{p}\cdot(\nabla\rho)$ in Eq. (5), dependent of the local density of adhesive bonds, $A(x,y;t)$. One can assume a dependence $\alpha \to \alpha(A) \simeq \alpha_0 A$ – an increase in the amount of adhesive bonds directly increases the force of propulsion. Note, however, that for too strong adhesion, the cell speed decreases again [36] – breaking of an adhesive bond takes too much energy, which could be captured by a non-monotonic function $\alpha(A)$. A continuous equation for the density of adhesive bonds (cf. also [25] for a discrete implementation of adhesion) can be written as [26]

$$\partial_t A = D_A \Delta A + \rho\left(a_0 p^2 + a_{nl} A^2\right) - \left(d(u) + sA^2\right) A\,. \tag{7}$$

In order of appearance, the terms on the r.h.s. describe diffusion, attachment and detachment/limitation of adhesive bonds. Note the simple implementation rules: formation of adhesive bonds should be restricted to the interior of the cell, hence the common factor of ρ. It has a linear contribution – proportional to p^2, guaranteeing the presence of actin. The nonlinear term models the fact that several mechanisms facilitate attachment of additional bonds if a bond has been already formed (for instance, locally reduced membrane fluctuations). The detachment rate $d(u)$ depends on the substrate displacement $\mathbf{u}(x,y;t)$ (or alternatively on the elastic restoring force). The cubic term limits the local density and is the simplest implementation of an excluded volume constraint (alternatively one could, in addition to the engaged bonds, add an equation for non-engaged bonds).

An equation governing the local substrate displacement $\mathbf{u}(x,y;t)$ can be obtained from linear elasticity theory in thin layer approximation [27] and is of the form

$$\partial_t \mathbf{u} = -\frac{1}{\eta}\left(G\mathbf{u} - \frac{1}{\xi}\left(\mathbf{T} + h\big[5\Delta\mathbf{T} + 19\nabla(\nabla\cdot\mathbf{T})\big]\right)\right). \tag{8}$$

Here G is the elastic modulus of the substrate, η describes dissipation in the adhesive layer and $\mathbf{T} = -\xi A\rho\left(\mathbf{p} + \frac{\langle A\mathbf{p}\rho\rangle}{\langle A\rho\rangle}\right)$ is the traction force exerted by the cell. It is proportional to both ρ (restriction to the interior) and A. The first traction contribution is opposite to the local propulsion direction $\mathbf{p}$, the second contribution is due to friction, and ξ describes the efficiency of force transmission [27]. Note that the total traction $\langle\mathbf{T}\rangle = \int \mathbf{T} dx\, dy = 0$ is zero, as it should be for a force-free self-propelled object. It is also possible to simplify the system by a projection on the force dipole in the direction of motion, leading to an effective equation for an overall (cell-averaged) substrate displacement $\mathbf{U}$ like $\frac{d}{dt}\mathbf{U} = -\frac{1}{\eta}\left(G\mathbf{U} + \mathbf{V}\right)$, where $\mathbf{V}$ is the center-of-mass velocity of the cell [26].

The model refinement discussed here reproduces many generic features observed experimentally for crawling cells, for instance the occurrence of stick-slip [37] and more complex motion (like bipedal motion of keratocytes [38]), confinement by adhesion [39] and stiffness [40] patterns, as well as durotactic motion [41] towards an optimum stiffness (i.e. substrate modulus). Figure 2 displays two examples of these features, not present in the simple model discussed in the previous section: panels a) and b) show typical traction force and substrate displacement patterns, that are consistent with generic features of traction force microscopy data for crawling cells, e.g. a maximum of traction at the front. Panel c) shows a prediction for the response of a moving cell on modulations of substrate properties, mimicking durotaxis: cells (only trajectories are shown) were prepared at different positions with respect to a stiffness gradient, modeled by a linear profile in G, cf. Eq. (8), and shown color-coded as black (soft) to

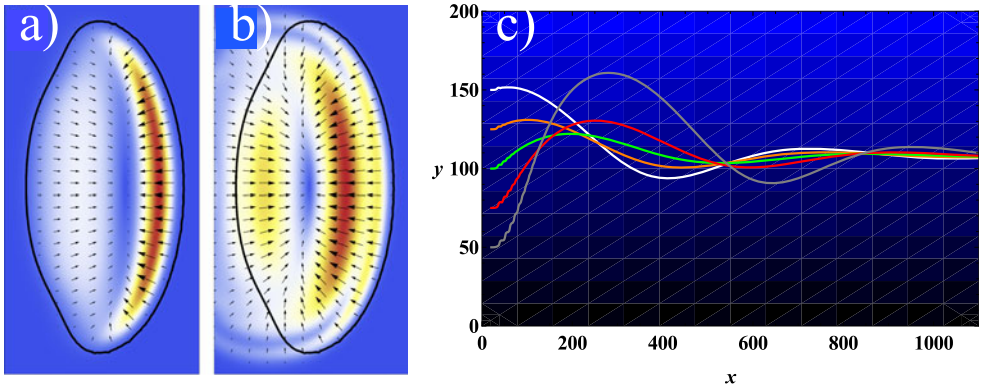

Fig. 2. Illustration of traction and displacement fields generated by a moving cell. (a) The traction force $\mathbf{T}$. Red (blue) corresponds to large (small) values of $|\mathbf{T}|$. (b) The displacement field $\mathbf{u}$. Red (blue) corresponds to large (small) values of $|\mathbf{u}|$. (c) Illustration of durotaxis: a linear gradient in the substrate's modulus G is implemented in the y-direction: $G = 0$ (black) at the bottom to $G = 0.4$ (blue) at the top. Colored curves show trajectories of cells for different initial positions. The trajectories converge to an optimal value of G. From [27].

blue (stiff) in the figure. In the course of time the cells select a region with an optimal stiffness. For more details we refer to [27].

This example shows the modularity of the modeling concept: Eqs. ((5), (6)) [including the motor-related terms discussed afterwards in Sect. 2] had not to be changed in the extended model, with the exception of the simple relation $\alpha \to \alpha_0 A$.

3.2 Possible complexity related to the cell membrane

The simple implementation of the cell's interface, Eq. (1), does not exhibit the proper elastic properties of a cell membrane. So far, it only has a wall energy (as known from the Ginzburg-Landau theory) that assures the tanh-form of the interface and represents an effective surface tension. In order to investigate specific membrane effects on cell motility, the description of the interface has to be refined. While cell membranes are complex objects, substantial work has been recently devoted to the phase field descriptions of (simpler) vesicles, e.g. in flows, including the following features:

Bending energy. Bending of the membrane can be directly accounted for within the phasefield approach [22,42] and has been included in the phase field model for motile cells in [23]. Its effect has not yet been thoroughly studied, but for a 2D description of a lamellipodium it should be rather negligible due to the typically large radius of curvature (of the order of 10 μm). It will become important, however, for 3D descriptions [43], where the thickness of the lamellipodium (some 200 nm) implies a radius of curvature of the order of 100 nm.

Surface tension. Vesicles have a practically vanishing surface tension. Hence in their phase field implementation, it is important to correct for the presence of the Ginzburg-Landau wall energy by a term $\propto C|\nabla\rho|$, where C is the local curvature [22,44,45]. In contrast to vesicles, cells have an effective (and non-constant) surface tension, which is still poorly understood and may depend on the cell's area, established adhesive bonds and their connection to the cytoskeleton, motors, etc. [46]. Since currently there is no model accounting for this complexity, and since the interface width (determined by D_ρ) is a somewhat artificial parameter, one can roughly

associate D_ρ to the effective surface tension (and neglect the correction needed for vesicles).

There is, however, one specific membrane property that may well be crucial: **Membrane inextensibility.** A (fluid) membrane is very hard to stretch, i.e. should be locally inextensible. Associated with this constraint is a Lagrangian multiplier (related to membrane tension), a quantity that is, in addition, accessible experimentally e.g. by micropipette aspiration. It has been recently suggested [19], that the membrane tension is important for determining the cell's shape: namely, membrane tension represents a restoring force against which the actin filaments have to push while polymerizing. If the tension is too high (beyond the so-called stall force for polymerization), no protrusion is possible. It has been argued that, via this mechanism, a resulting graded distribution of actin might be responsible for the elongated canoe-like shape of keratocytes. Membrane tension has also been recently shown to be an important factor for crawling sperm cells of *C. Elegans* [47].

Within the phase field approach, tension leads to an additional force due to the membrane in the internal dynamics equation. Denoting the Lagrangian multiplier with $\zeta(x, y; t)$, local curvature with C, and introducing the local normal and tangent unit vectors, $\hat{\mathbf{n}} = \frac{\nabla\rho}{|\nabla\rho|}$ and $\hat{\mathbf{t}} = \hat{\mathbf{n}} \times \hat{\mathbf{e}}_z$, respectively, this force can be written as [22,45]

$$\mathbf{f}_{tens} = \zeta C \hat{\mathbf{n}} + \hat{\mathbf{t}} \cdot \nabla\zeta \hat{\mathbf{t}} \quad \text{with} \quad C = -\nabla \cdot \hat{\mathbf{n}} \,. \tag{9}$$

The Lagrangian multiplier itself (stemming from the condition $\int \zeta dl = \text{const.}$ along the membrane's 2D contour) evolves according to [22,45]

$$\partial_t \zeta = -\mathbf{v} \cdot \nabla\zeta + T\hat{\mathbf{t}} \cdot (\hat{\mathbf{t}} \cdot \nabla)\mathbf{v} \,. \tag{10}$$

Here $\mathbf{v}$ is the predominant local velocity. For vesicles, it typically is given by Stokes flow. In our case, $\mathbf{v} \propto \mathbf{p}$ due to actin polymerization, but it could also be the actin flow field, if it is accounted for explicitly (cf. the discussion in the next section). T is the stiffness of the tension constraint, with units of force per length.

The main feature of the tension within our model will be the following: the force given in Eq. (9) adds a term $\mathbf{f}_{tens}|\nabla\rho|$ to the equation for the actin polarization $\mathbf{p}$. Hence it counteracts the polymerization term $-\beta\nabla\rho$, as it should, and self-consistently yields a certain force-velocity relation. Apart from that, since α, β are coarse-grained parameters related to the actin polymerization kinetics, one could in addition allow for $\alpha \to \alpha(\zeta)$ and $\beta \to \beta(\zeta)$. However, in contrast to molecular motors acting against a force, unfortunately the force-velocity relation of the – usually highly collective – polymerization of actin against a force is not yet well understood. So far it is only known to be fairly constant for low forces and then dropping abruptly to zero close to the stall force [48–50]. If better data, especially for moving cells, becomes available, the tension and its effect on the overall velocity and the cell's shape will become worthwhile to be investigated further.

Apart from being more realistic, a technical feature of the inclusion of membrane tension is that the explicit volume conservation in $\delta[\rho]$ is no longer needed, i.e. Eq. (4) can be simplified to $\delta = \frac{1}{2} - \sigma|\mathbf{p}|^2$ (if motor contraction is included). In other words, accounting for the additional Eq. (10) and the concomitant force renders the simple model *local*. Note however that, if considered, traction still induces nonlocal effects.

4 Diverse motility mechanisms can be modeled by different internal dynamics modules

As discussed earlier, the three crucial "steps" during cell motion, as identified by Abercrombie [1], are protrusion, adhesion and force transfer, and finally retraction.

These processes are employed and expressed in different ways by different cell types, e.g. fibroblasts, keratocytes, and neutrophils. Here we discuss how one could include cell-type specific behavior, as well as motility modes different from the "Abercrombie steps", in the self-consistent phase field modeling framework.

Fibroblasts. The crawling motion of fibroblasts is very different from that of keratocytes in at least two respects: first, fibroblast cells are much slower, allowing adhesion sites to mature under cortical stress [8]. Second, the resulting shape is fan-like [51] with the arc-like interfaces at the front due to the balance of actin fibers between focal adhesions and an effective surface/line tension. The latter is quite similar to a model proposed for stationary, spreading cells by Bischofs et al. [52]: there the cell shape has been described by the balance of the effective line tension λ along the contour with the adhesion tension f_{ad} from the (discrete or continuous) adhesion sites located at positions $\mathbf{r}_{ad}$ close to the cell's boundary, $\int \lambda dl = \int \mathbf{f}_{ad} \cdot (\mathbf{r} - \mathbf{r}_{ad}) dl$. Note that this effect can be incorporated in the refined cell membrane description discussed in the last section.

Due to the much stronger adhesion compared to keratocytes, modeling fibroblast motion in addition needs an explicit implementation of internal stresses. A good starting point in this respect will be the continuum theory of "active gels", established by Kruse et al. [31,53]. There the generic hydrodynamics (including possible viscoelasticity, cf. also [32]) of bulk active polar gels was developed. In addition to classical stress contributions – pressure, viscous stresses, Erickson stresses due to liquid crystalline order – the active stress $\sigma_{ij}^A = \zeta \Delta\mu (p_i p_j - \frac{1}{2} p^2)$ was introduced, where $\mathbf{p}$ is the coarse-grained actin orientation, $\Delta\mu$ the chemical energy delivered by the ATP hydrolysis, and ζ a phenomenological coefficient. Note that the principal value of this tensor was used by us in the simple model discussed in Sect. 2 to describe actomyosin contraction. Adding the generalized (Navier-)Stokes equation for the actin velocity to the equation for $\mathbf{p}$, cytoskeleton-related stresses will be self-consistently accounted for (cf. also a related study of active gel droplets [54]). In addition, however, these stresses will generate a feedback to the adhesion via stress-induced maturation. The only model we are aware of that attempted to treat this interplay is the one by Stéphanou et al. [55]: there adhesion points, focal complexes and focal adhesions were accounted for, where only the former are formed spontaneously and only the latter contribute to cell motion. Transitions between these stages occur under stresses between the cell body and the membrane, stemming from actin fibers. While giving rise to irregular motion and correct relations between the cell speed and cell area, for instance, the shapes did not resemble fibroblasts and where not substantially perturbed from round.

Concluding, combination of the line tension-adhesion balance implemented into the phase field interface (to model the fan-like shape) with explicit stresses (the Navier-Stokes-type equation for the active gel) and stress-induced adhesion maturation (similar to [55]), would be a promising, but obviously quite challenging, modeling framework for fibroblasts and related slowly moving cells.

Chemotactic motion of amoebae. The irregular motion of amoebae, typically with special focus on their chemotactic behavior, is usually modeled by reaction diffusion equations that have consequences only at the interface, cf. the recent review [18]. Current works are typically using three equations, one for the activator and two for the inhibitors, one global and one local (inspired by [56]), and both phase field [57] and level set [58] methods have been applied to this system. However, protrusions where so far only modeled as, e.g. curvature, changes stimulated by the reaction-diffusion module: i.e. the interplay between sensing and stimulation with the underlying actin cytoskeleton – that actually causes the local pseudopod protrusions – has not yet been modeled systematically. This is obviously at reach by combining the simple approach discussed in Sect. 2 (or alternatively including stresses/flow as discussed just above)

with a suitable reaction diffusion system. The latter can easily be confined to the interface, as already discussed, by implementing the reactant equations with factors $(\nabla\rho)^2$.

Nematode sperm. Spermatozoa from nematodes like *A. suum* and *C. elegans* are attractive model systems as their motility apparatus is much simpler than for crawling epithelial cells: namely, instead of an actin cytoskeleton nematode sperm cells contain a polymerized network of major sperm protein (MSP), and to date there are no motors known associated to that cytoskeletal network. Locally the motility is amoebae-like (i.e. via protrusions) but the overall shape is elongated along the direction of motion – probably due to the absence of motor-induced contractile forces. Modeling efforts [10,59] are based on the swelling (at the front) and contraction (at the rear) of the gel-like MSP-network; a continuum version of the propulsion by a swelling gradient was also presented in [6]. Full models including the self-consistent description of the elongated shape, however, are missing.

Within our framework, one can omit the **p**-field – note that MSP is not polar – and rather consider the stress field of the network (cf. the discussion for fibroblasts above). While motor contraction stresses will be absent, active stresses due to polymerization of the gel are still present. In addition, the stress will depend on the local volume fraction of the gel, $\sigma = \sigma(\phi)$, with ϕ the volume fraction [6,10]. Important questions are, for instance, related to the establishment of the elongated shape and the retrograde flow, and to the effects of membrane tension on cell shape and speed, as studied recently experimentally [47].

Propulsion by polymerization waves. In contrast to more (like for keratocytes) or less (like for fibroblasts) steady cell motion, amoeboidal motion (occurring also for neutrophils) is characterized by protrusions that apparently randomly form along the cell periphery and drive the cell forward. It is long known that these (non-chemotactic) protrusions are the result of local polymerization of the actin cytoskeleton. Quite recently, it has been shown that *polymerization waves* can emerge spontaneously from the interaction of actin filaments and nucleation promoting factors (NPFs) [4,60–63]. The effect of cytoskeletal polymerization waves on cell migration has been already discussed, e.g. in [64,65]. It can also be conveniently implemented in the phase-field description discussed here, by coupling the equations for the phase field and for the orientation of the actin network, **p**, to suitable rate equations for the densities of active and inactive NPFs. Employing this route, the study [66] reports, in addition to possible directional motion, states reminiscent of the protrusion-mediated amoeboid motility. The analysis of the model shows that new protrusions emerge from a nucleation process in the cell's interior that generate actin spiral waves. Note that this process does not require (explicit) noise; rather it occurs in a dynamic state displaying spatio-temporal chaos, similar as discussed in [67].

Generic features of active stress-induced propulsion. Several analytical studies have discussed generic features of the propulsion by active stresses, cf. [68] and references therein. For example, recently the difference between pushing and pulling for a crawling cell has been studied in Ref. [5], including non-trivial force-velocity relations. Such and related general questions – that have not yet been addressed in full motile cell models, due to the complexity of the latter – could be treated within our framework. As the underlying studies are typically 1D and consider the cell boundary simply as a wall, a suitable implementation in the phase-field framework could test the robustness of the predictions against (self-induced) deformations of the cell's shape.

Biomimetic systems. There are increasing efforts to develop biomimetic "cells" and artificial "crawlers". Several groups are currently trying to encapsulate actomyosin into giant vesicles with embedded membrane proteins that could interact with actin. Related to these efforts, but obviously more artificial, Sanchez et al. [69] recently reported on a microtubule-motor solution encapsulated in oil droplets. These could

propel themselves (in solution) due to chaotic internal dynamics. Note the similarity to the propulsion by spatio-temporal chaos related to actin polymerization [66].

On the other hand, there is growing effort to develop purely synthetic artificial crawlers [70]. One approach [71] relies on nanoparticle-filled microcapsules placed on an adhesive substrate. Such capsules can display self-sustained motion, since the permeability of their shell depends on mechanical deformation: in turn, the capsules release nanoparticles that bind to the surface and dynamically create an adhesion gradient, causing them to move autonomously from regions of less adhesion to larger adhesion. The motion is self-sustained, until the capsules are depleted of nanoparticles. This system has already been treated with a phase-field approach very similar to the one discussed here [72], with the gradient ∇c of the nanoparticle concentration playing the role of the propulsion force $\mathbf{p}$.

5 Conclusions

We have discussed here an efficient yet very simple approach to model cell motion. The phase field description for the cell's moving boundary circumvents one of the major (numerical, but also conceptional) bottlenecks. Then we discussed on how this approach can be extended in a modular way to increase the level of description, and how different specific cell types could be modeled within a single, unified framework. We have also made a point on how conveniently one can couple internal constituents/effects, as well as effects confined to the proximity of the cell membrane, into the modeling.

It should be noted that the literature in modeling cell motility is currently expanding very rapidly. Understandably, however unfortunately, the methods employed *and* the effects treated are often quite different. In turn, this makes comparisons between different models and research groups very difficult, cf. also the discussion in the recent review [18]. The conceptual simplicity of the proposed approach might help to achieve such important comparisons and establish a unified framework for modeling the motion of different cell types, as well as of related biomimetic objects. Note that the phase field approach would also facilitate the description of motion of cell layers, as occurring e.g. during development or during wound closing [73].

Finally, on the one hand the modular approach could bridge the gap between simple 1D or fixed shape models and some very complex, partially 3D, approaches that have been started to be developed already some time ago but due to their complexity could not be studied in much detail [74,75]. On the other hand, generic features are currently established by even more coarse-grained models, cf. [76], that could be tested within a more realistic, i.e. specific, context.

References

1. M. Abercrombie, Proc. R. Soc. London B **207**, 129 (1980)
2. D. Bray, *Cell movements: from molecules to motility* (Garland Pub, 2001)
3. C.S. Peskin, G.M. Odell, G.F. Oster, Biophys. J. **65**, 316 (1993)
4. K. Doubrovinski, K. Kruse, EPL **83**(1), 18003 (2008)
5. P. Recho, L. Truskinovsky, Phys. Rev. E **87**, 022720 (2013)
6. J.F. Joanny, F. Jülicher, J. Prost, Phys. Rev. Lett. **90**, 168102 (2003)
7. K. Burridge, M. Chrzanowska-Wodnicka, Ann. Rev. Cell Dev. Biol. **12**, 463 (1996)
8. U.S. Schwarz, M.L. Gardel, J. Cell Sci. **125**, 3051 (2012)
9. J. Renkawitz, K. Schumann, M. Weber, T. Lämmermann, H. Pflicke1, M. Piel, J. Polleux, J. Spatz, M. Sixt, Nature Cell Biol. **11**, 1438 (2009)

10. C.W. Wolgemuth, L. Miao, O. Vanderlinde, T. Roberts, G. Oster, Biophys. J. **88**, 2462 (2005)
11. P.T. Yam, C.A. Wilson, L. Ji, B. Hebert, E.L. Barnhart, N.A. Dye, P.W. Wiseman, G. Danuser, J.A. Theriot, J. Cell Biol. **178**, 1207 (2007)
12. U. Euteneuer, M. Schliwa, Nature **310**, 58 (1984)
13. A.B. Verkhovsky, T.M. Svitkina, G.G. Borisy, Curr. Biol. **9**, 11 (1999)
14. J. Lee, A. Ishihara, J.A. Theriot, K. Jacobson, Nature **362**, 167 (1993)
15. H. Grimm, A. Verkhovsky, A.M. A, J. Meister, Eur. Biophys. J. **32**, 563 (2003)
16. K. Kruse, J.F. Joanny, F. Jülicher, J. Prost, Phys. Biol. **3**, 130 (2006)
17. M.M. Kozlov, A. Mogilner, Biophys. J. **93**, 3811 (2007)
18. W.R. Holmes, L. Edelstein-Keshet, PLoS Comp. Biol. **8**, e1002793 (2012)
19. K. Keren, Z. Pincus, G.M. Allen, E.L. Barnhart, G. Marriott, A. Mogilner, J.A. Theriot, Nature **453**, 475 (2008)
20. I.S. Aranson, V.A. Kalatsky, V.M. Vinokur, Phys. Rev. Lett. **85**, 118 (2000)
21. A. Karma, W.J. Rappel, Phys. Rev. E **57**, 4323 (1998)
22. T. Biben, C. Misbah, Phys. Rev. E **67**, 031908 (2003)
23. D. Shao, W.J. Rappel, H. Levine, Phys. Rev. Lett. **105**, 108104 (2010)
24. F. Ziebert, S. Swaminathan, I.S. Aranson, J.R. Soc. Interface **9**, 1084 (2012)
25. D. Shao, H. Levine, W.J. Rappel, Proc. Natl. Acad. Sci. USA **109**, 6851 (2012)
26. F. Ziebert, I.S. Aranson, PLOS ONE **8**, e64511 (2013)
27. J. Löber, F. Ziebert, I.S. Aranson, Soft Matt. **10**, 1365 (2014)
28. W. Marth, A. Voigt, J. Math. Biol.; published online (2013); doi:10.1007/s00285-013-0704-4
29. C.W. Wolgemuth, J. Stajic, A. Mogilner, Biophys. J. **101**, 545 (2011)
30. D.A. Kessler, J. Koplik, H. Levine, Adv. Phys. **37**(3), 255 (1988)
31. K. Kruse, J.F. Joanny, F. Jülicher, J. Prost, K. Sekimoto, Eur. Phys. J. E **16**, 5 (2005)
32. B. Rubinstein, M.F. Fournier, K. Jacobson, A.B. Verkhovsky, A. Mogilner, Biophys. J. **97**, 1853 (2009)
33. H.R. Brand, H. Pleiner, F. Ziebert, Phys. Rev. E **74**, 021713 (2006)
34. M. Dembo, Y.L. Wang, Biophys. J. **76**, 2307 (1999)
35. M.F. Fournier, R. Sauser, D. Ambrosi, J.J. Meister, A.B. Verkhovsky, J. Cell Biol. **188**, 287 (2010)
36. S.P. Palecek, J.C. Loftus, M.H. Ginsberg, D.A. Lauffenburger, A.F. Horwitz, Nature **385**, 537 (1997)
37. T.A. Ulrich, E.M. de Juan Pardo, S. Kumar, Cancer Res. **69**, 4167 (2009)
38. E. Barnhart, G. Allen, F. Jülicher, J. Theriot, Biophys. J. **98**(6), 933 (2010)
39. C.G. Rolli, H. Nakayama, K. Yamaguchi, J. Spatz, R. Kemkemer, J. Nakanishi, Biomaterials **33**, 2409 (2012)
40. L. Trichet, J. Le Digabel, R.J. Hawkins, S.R.K. Vedula, M. Gupta, C. Ribrault, P. Hersen, R. Voituriez, B. Ladoux, Proc. Natl. Acad. Sci. USA **109**, 6933 (2012)
41. C.M. Lo, H.B. Wang, M. Dembo, Y.L. Wang, Biophys. J. **79**, 144 (2000)
42. J.S. Lowengrub, A. Rätz, A. Voigt, Phys. Rev. E **79**, 031926 (2009)
43. M. Herant, M. Dembo, Biophys. J. **98**, 1408 (2010)
44. R. Folch, J. Casademunt, A. Hernandez-Machado, L. Ramirez-Piscina, Phys. Rev. E **60**, 1724 (1999)
45. J. Beaucourt, F. Rioual, T. Séon, T. Biben, C. Misbah, Phys. Rev. E **69**, 011906 (2004)
46. T. Lecuit, P.F. Lenne, Nature Rev. Mol. Cell Biol. **8**, 633 (2007)
47. E.L. Batchelder, G. Hollopeter, C. Campillo, X. Mezanges, E.M. Jorgensen, P. Nassoy, P. Sens, J. Plastino, Proc. Natl. Acad. Sci. USA **108**, 11429 (2011)
48. S.H. Parekh, O. Chaudhuri, J.A. Theriot, D.A. Fletcher, Nature Cell Biol. **7**, 1219 (2005)
49. M. Prass, K. Jacobson, A. Mogilner, M. Radmacher, J. Cell Biol. **174**, 767 (2006)
50. J. Zimmermann, C. Brunner, M. Enculescu, M. Goegler, A. Ehrlicher, J. Käs, M. Falcke, Biophys. J. **102**, 287 (2012)
51. A. Mogilner, K. Keren, Curr. Biol. **19**, R762 (2009)
52. I. Bischofs, S. Schmidt, U. Schwarz, Phys. Rev. Lett. **103**, 048101 (2009)

53. K. Kruse, J.F. Joanny, F. Jülicher, J. Prost, K. Sekimoto, Phys. Rev. Lett. **92**, 078101 (2004)
54. E. Tjhung, D. Marenduzzo, M.E. Cates, Proc. Nat. Acad. Sci. USA **109**, 12381 (2012)
55. A. Stéphanou, E. Mylona, M. Chaplain, P. Tracqui, J. Theoret. Biol. **253**, 701 (2008)
56. H. Meinhardt, J. Cell Sci. **112**, 2867 (1999)
57. H. Levine, D. Kessler, W.J. Rappel, Proc. Natl. Acad. Sci. USA **103**, 9761 (2006)
58. C. Shi, C.H. Huang, P. Devreotes, P. Iglesias, PLoS Cell Biol. **9**, e1003122 (2013)
59. D. Bottino, A. Mogilner, T. Roberts, M. Stewart, G. Oster, J. Cell Sci. **115**, 367 (2002)
60. H. Le Guyader, C. Hyver, C. R. Acad. Sci. Paris. Life Sci. **320**(1), 59 (1997)
61. O.D. Weiner, W.A. Marganski, L.F. Wu, S.J. Altschuler, M.W. Kirschner, PLoS Biol. **5**, e221 (2007)
62. S. Whitelam, T. Bretschneider, N.J. Burroughs, Phys. Rev. Lett. **102**, 1 (2009)
63. A.E. Carlsson, Phys. Rev. Lett. **104**, 228102 (2010)
64. K. Doubrovinski, K. Kruse, Phys. Rev. Lett. **107**, 258103 (2011)
65. D. Taniguchi, S. Ishihara, T. Oonuki, M. Honda-Kitahara, K. Kaneko, S. Sawai, Proc. Nat. Acad. Sci. USA **110**, 5016 (2013)
66. A. Dreher, I.S. Aranson, K. Kruse (submitted) (2013)
67. I. Aranson, H. Levine, L. Tsimring, Phys. Rev. Lett. **76**, 1170 (1996)
68. A.E. Carlsson, New J. Phys. **13**, 073009 (2011)
69. T. Sanchez, D.T.N. Chen, S.J. DeCamp, M. Heymann, Z. Dogic, Nature **491**, 431 (2012)
70. D.A. Hammer, G.P. Robbins, J.B. Haun, J.J. Lin, W. Qi, L.A. Smith, P. Ghoroghchian, M.J. Therien, F.S. Bates, Faraday Discuss. **139**, 129 (2008)
71. K. Kratz, A. Narasimhan, R. Tangirala, S. Moon, R. Revanur, S. Kundu, H. Kim, A. Crosby, T. Russell, T. Emrick, et al., Nature Nanotech. **7**, 87 (2012)
72. G.V. Kolmakov, A. Schaefer, I. Aranson, A.C. Balazs, Soft Matt. **8**, 180 (2012)
73. M.H. Köpf, L.M. Pismen, Soft Matt. **9**, 3727 (2013)
74. W. Alt, M. Dembo, Math. Biosci. **156**, 207 (1999)
75. E. Kuusela, W. Alt, J. Math. Biol. **58**, 135 (2009)
76. T. Ohta, T. Ohkuma, Phys. Rev. Lett. **102**, 154101 (2009)